The Effect of Postmastectomy Radiation Therapy on Breast Implants

Material Analysis on Silicone and Polyurethane Prosthesis

Federico Lo Torto, MD, Michela Relucenti, BSc, PhD,† Giuseppe Familiari, MD,† Nicola Vaia, MD,* Donato Casella, PhD,‡ Roberto Matassa, PhD, EBM,† Selenia Miglietta, BSc, PhD,† Franco Marinozzi, PhD,§ Fabiano Bini, PhD,§ Ilaria Fratoddi, PhD,|| Fabio Sciubba, PhD,|| Raffaele Cassese, MD,¶ Vincenzo Tombolini, MD,¶ and Diego Ribuffo, MD**

Introduction: The pathogenic mechanism underlying capsular contracture is still unknown. It is certainly a multifactorial process, resulting from human body reaction, biofilm activation, bacteremic seeding, or silicone exposure. The scope of the present article is to investigate the effect of hypofractionated radiotherapy protocol (2.66 Gy × 16 sessions) both on silicone and polyurethane breast implants.
Methods: Silicone implants and polyurethane underwent irradiation according to a hypofractionated radiotherapy protocol for the treatment of breast cancer. After irradiation implant shells underwent mechanical, chemical, and microstructural evaluation by means of tensile testing, infrared spectra in attenuated total reflectance mode, nuclear magnetic resonance, and field emission scanning electron microscopy.
Results: At superficial analysis, irradiated silicone samples show several visible secondary and tertiary blebs. Polyurethane implants showed an open cell structure, which closely resembles a sponge. Morphological observation of struts from treated polyurethane sample shows a more compact structure, with significantly shorter and thicker struts compared with untreated sample. The infrared spectra in attenuated total reflectance mode spectra of irradiated and control samples were compared either for silicon and polyurethane samples. In the case of silicone-based membranes, treated and control specimens showed similar bands, with little differences in the treated one. Nuclear magnetic resonance spectra on the fraction soluble in CDCl3 support these observations. Tensile tests on silicone samples showed a softer behavior of the treated ones. Tensile tests on Polyurethane samples showed no significant differences.
Conclusions: Polyurethane implants seem to be more resistant to radiotherapy damage, whereas silicone prosthesis showed more structural, mechanical, and chemical modifications.

Key Words: breast, implants, mastectomy, polyurethane implants, reconstruction, radiotherapy, silicone implants

(*Ann Plast Surg* 2018;00: 00–00)

Postmastectomy radiation therapy (PMRT) is shown to decrease local recurrence and improve survival rate in patients with 4 or more positive axillary lymph nodes and in patients with tumors larger than 5 cm. Several studies are now expanding PMRT indications, including patients with stage II cancers and less than 4 involved nodes.[1,2] Standard fractionated chest wall radiotherapy uses 2-Gy daily fractions for up to 6 weeks of treatment. Over the past decade, the use of hypofractionated radiotherapy, which consists of delivering higher dose per fraction for shorter number of sessions (2.66 Gy × 16 sessions), is widely increasing. It is well known that radiation therapy leads to a higher risk of capsular contracture causing breast distortion, pain, and unsatisfactory aesthetic outcome.[3,4] The pathogenic mechanism underlying capsular contracture is still unknown. It is certainly a multifactorial process, resulting from human body reaction, biofilm activation, bacteremic seeding, or silicone exposure.[5,6] Indeed, while the nature of radiation effects on soft tissues has been deeply investigated, only few studies have examined radiation effects on breast implants.[7–9] We previously described the effect of PMRT on breast implant surface addressing morphological and chemical alterations of silicone breast implants exposed to the conventional protocol of radiotherapy (2 Gy × 25 sessions).[10] The aim of the present article was to investigate the effect of hypofractionated radiotherapy protocol (2.66 Gy × 16 sessions) both on silicone and polyurethane breast implants.

Received December 6, 2017, and accepted for publication, after revision February 27, 2018.
From the *Plastic Surgery Unit, Department of Surgery "P. Valdoni" Sapienza University Rome, Italy; †Department of Human Anatomy, Histology, Forensic Medicine and Orthopaedics Section of Human Anatomy Electron Microscopy Unit, Laboratory "Pietro M. Motta" Faculty of Pharmacy and Medicine, University of Rome La Sapienza; ‡Breast Unit, Department of Oncologic and Reconstructive Breast Surgery, "Breast Unit Integrata di Livorno, Cecina, Piombino, Elba, Azienda USL Toscana Nord Ovest"; and §Department of Mechanical and Aerospace Engineering, "Sapienza" University of Rome; ||Department of Chemistry, Sapienza University of Rome; and ¶Department of Radiation Oncology, "Sapienza" University of Rome, Rome, Italy.
Conflicts of interest and sources of funding: none declared.
Reprints: Nicola Vaia, MD, Sapienza University of Rome, Rome, Italy. E-mail: Nicola.vaia@gmail.com.

ISSN: 0148-7043/18/0000–0000
DOI: 10.1097/SAP.0000000000001461

METHODS AND MATERIALS

Textured medical grade silicone implants (260 mL Memè TMP) and polyurethane (435 mL Replicon MXP) implants were kindly provided by Polytech (Polytech Health & Aesthetics GmbH, Dieburg, Germany). The breast implants were wrapped in a shell that simulated the characteristics of the surrounding soft tissue (ExaFlex Bolus) with a thickness of 1 cm and density comparable to the skin and subcutaneous tissue (1.03 g/cm). The Bolus has been perfectly adhered to the prosthesis to avoid the presence of air spaces that would modify the dose distribution[10,11] and underwent irradiation according to a hypofractionated radiotherapy protocol for the treatment of breast cancer. The protocol consisted of a total radiation dose of 42.56 Gy, fractioned into 16 treatments. Nonirradiated prostheses of comparable size were used as a control.

Surface Analysis

From the domed area of each implant, shell samples of approximately 1 cm^2 were randomly collected through the use of scissors.

Specimen morphology was characterized by field emission scanning electron microscopy (FE Hitachi S4000, Japan). Samples were mounted on aluminum stubs using adhesive carbon tape and then sputter coated with a conductive layer of platinum (Emitech K550 sputter coating). Silicone samples were observed at an accelerating voltage of 5 kV; polyurethane samples were observed at an accelerating voltage of 20 kV.

Infrared spectra in attenuated total reflectance mode (ATR-FTIR) spectra have been recorded on solid samples with a Bruker Vertex 70 spectrophotometer.

Nuclear magnetic resonance (NMR) spectra were recorded in $CDCl_3$ and D_2O at 298 K on a Bruker AVANCE III spectrometer at 9.4 T operating at the hydrogen frequency of 400.13 MHz and equipped with a Bruker multinuclear z-gradient inverse probe head.

Mechanical Characterization

Tensile tests were executed on both treated and untreated samples with a tensile tester (Zwick/Roell Z010, Ulm, Deutschland). Dog-bone–shaped specimens were obtained from the shell of each breast implant. In accordance with Yildirimer et al,[12] an extension rate of 100 mm/min was selected. The samples were stretched until rupture while recording stress-strain curves. The elasticity modulus (E_{mod}) was computed according to ASTM standards for each sample using the linear tract of the stress-strain curve (*t*). Breaking strength and strain were also recorded. Experiments were performed in triplicate.

Statistical Analysis

Data analysis was performed using MedCalc software (Ostend, Belgium). Conditions of normality were checked using D'Agostino-Pearson test. Differences between treated and control groups were assessed using either paired-sample *t* test (for normally distributed data) or Mann-Whitney *U* nonparametric test (for data not following normal distribution). Ten different microscopic fields at a 30× magnification were acquired for each group. For silicone samples, average roughness (R_a, arithmetic average deviation from the mean line) and kurtosis (R_{ku}, a measure of the distribution of spikes above and below the mean line) were calculated. For spiky surfaces, R_{ku} is greater than 3; for bumpy surfaces, R_{ku} is less than 3; perfectly random surfaces have kurtosis of 3. Skewness (R_{sk}) were calculated by Fiji free software, using roughness calculation plug-in (R_{sk} is a measure of the asymmetry of the profile about the mean line; negative skew indicates a predominance of valleys, whereas positive skew is seen on surfaces with peaks).

For the polyurethane sample, open cell pore size and interconnection dimensions were calculated with Fiji free software, using Analyze → Measurement function.

RESULTS

At superficial analysis, nontreated silicone samples appear as having a blebbing surface; more precisely, there are primary larger blebs on the top of which sometimes a small valley or a secondary small bleb is visible. Blebs' surface seems to be smooth.

Irradiated silicone samples, on the other hand, show a completely different aspect. On the top of the primary blebs are several visible secondary and tertiary blebs with heterogeneous dimensions that confer a very irregular aspect to the sample (Fig. 1).

Roughness analysis was carried out on images taken at the same magnification and kV in order to represent the same area in each photograph. The roughness parameters calculated were R_a, R_{ku}, and R_{sk}. The values of all these parameters measured in the normal and treated samples were statistically different. The R_a roughness parameter defines an average surface finish value; from the R_a value, it can be understood that the average profile in the treated samples is lower than the average

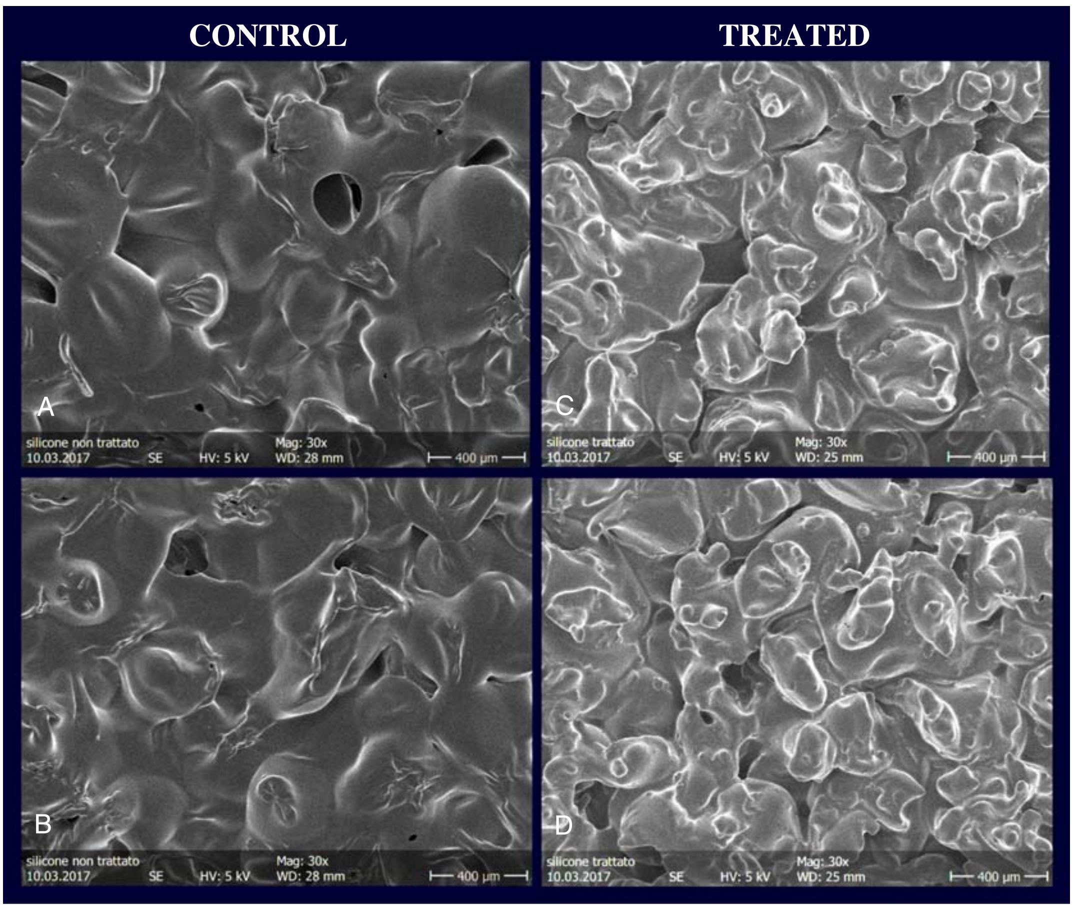

FIGURE 1. Field emission scanning electron microscopy of silicone samples. A and B, Control (untreated) silicone samples. C and D, Treated silicone samples.

TABLE 1. Silicone Sample Results and Statistical Analysis

R_a*	Arithmetic Mean	95% CI for the Mean	Median	95% CI for the Median	Variance	SD	SEM	Coefficient of Skewness	Coefficient of Kurtosis	D'Agostino-Pearson Test for Normal Distribution
Normal	88.0929	85.7380 to 90.4478	88.2935	85.4209–91.2253	10.8370	3.2920	1.0410	−0.4433 (P = 0.5057)	−0.3041 (P = 0.9563)	Accept normality (P = 0.8001)
Treated	78.1898	76.1858 to 80.1938	77.3420	75.5697 to 81.3568	7.8477	2.8014	0.8859	0.5329 (P = 0.4248)	−1.0423 (P = 0.4238)	Accept normality (P = 0.5281)

R_a*	Mean Difference	SD of Mean Difference	SE of Mean Difference	95% CI	t Test	Degrees of Freedom	2-Tailed Probability
Normal vs treated	−9.9031	4.4990	1.4227	−13.1215 to −6.6847	−6.961	9	P = 0.0001

R_{ku}†	Arithmetic Mean	95% CI for the Mean	Median	95% CI for the Median	Variance	SD	SEM	Coefficient of Skewness	Coefficient of Kurtosis	D'Agostino-Pearson Test for Normal Distribution
Normal	1.7088	1.6431 to 1.7745	1.6640	1.6419 to 1.8088	0.008436	0.09185	0.02905	0.8073 (P = 0.2310)	−0.6865 (P = 0.6782)	Accept normality (P = 0.4478)
Treated	2.2196	2.1599 to 2.2793	2.2575	2.1245 to 2.2885	0.006975	0.08352	0.02641	−0.4910 (P = 0.4615)	−1.6502 (P = 0.1073)	Accept normality (P = 0.2085)

R_{ku}†	Mean Difference	SD of Mean Difference	SE of Mean Difference	95% CI	t Test	Degrees of Freedom	2-Tailed Probability
Normal vs treated	0.5108	0.1174	0.03712	0.4268 to 0.5948	13.761	9	P < 0.0001

R_{sk}‡	Arithmetic Mean	95% CI for the Mean	Median	95% CI for the Median	Variance	SD	SEM	Coefficient of Skewness	Coefficient of Kurtosis	D'Agostino-Pearson Test for Normal Distribution
Normal	1.2112	1.1926 to 1.2298	1.1970	1.1935 to 1.2358	0.0006760	0.02600	0.008222	0.8210 (P = 0.2234)	− 0.5583 (P = 0.7728)	Accept normality (P = 0.4571)
Treated	1.3579	1.3426 to 1.3732	1.3660	1.3319 to 1.3756	0.0004603	0.02146	0.006785	−0.4213(P = 0.5268)	−1.6229 (P = 0.1167)	Accept normality (P = 0.2391)

R_{sk}‡	Mean Difference	SD of Mean Difference	SE of Mean Difference	95% CI	t Test	Degrees of Freedom	2-Tailed Probability
Normal vs treated	0.1467	0.03121	0.009870	0.1244 to 0.1690	14.863	9	P < 0.0001

Conditions of normality were checked using D'Agostino-Pearson test. Differences between treated and control groups were assessed using either paired-sample t test (for normally distributed data) or Mann-Whitney U nonparametric test (for data not following normal distribution).

*R_a is arithmetic average deviation from the mean line.

†R_{ku} is a measure of the distribution of spikes above and below the mean line. For spiky surfaces, $R_{ku} > 3$; for bumpy surfaces, $R_{ku} < 3$; perfectly random surfaces have kurtosis 3.

‡R_{sk} is a measure of the asymmetry of the profile about the mean line; negative skew indicates a predominance of valleys, whereas positive skew is seen on surfaces with peaks.

TABLE 2. Polyurethane Sample Results and Statistical Analysis

Pores Area	Arithmetic Mean	95% CI for the Mean	Median	95% CI for the Median	Variance	SD	SEM	Coefficient of Skewness	Coefficient of Kurtosis	D'Agostino-Pearson Test for Normal Distribution
Normal	29,012.8487	25,274.0497 to 32,751.6476	23,936.9805	19,035.8036 to 28,720.1548	398,717,073.7543	19,967.9011	1886.7893	0.9803	0.3089	Reject normality ($P = 0.0005$)
Treated	21,883.7735	18,989.2348 to 24,778.3123	21,565.0965	17,469.2778 to 25,368.4571	238,978,788.0458	15,458.9388	1460.7324	0.3181 ($P = 0.1594$)	−0.6975 ($P = 0.0311$)	Reject normality ($P = 0.00363$)

Area	Mann-Whitney *U*	*Z* Test	2-Tailed Probability
Normal vs treated	5127.50	2.360	$P = 0.0183$

Pores Perimeter	Arithmetic Mean	95% CI for the Mean	Median	95% CI for the Median	Variance	SD	SEM	Coefficient of Skewness	Coefficient of Kurtosis	D'Agostino-Pearson Test for Normal Distribution
Normal	622.3263	581.2132 to 663.4393	589.2685	526.1268 to 687.6921	48,212.5648	219.5736	20.7478	0.3123 ($P = 0.1668$)	−0.9073 ($P = 0.0007$)	Reject normality ($P = 0.0012$)
Treated	501.8222	457.0085 to 546.6359	557.1150	495.2178 to 609.4036	57,282.5912	239.3378	22.6153	−0.5730 ($P = 0.0147$)	−0.6019 ($P = 0.0867$)	Reject normality ($P = 0.0118$)

Perimeter	Mann-Whitney *U*	*Z* Test	2-Tailed Probability
Normal vs treated	4850.00	2.932	$P = 0.0034$

Struts Length	Arithmetic Mean	95% CI For The Mean	Median	95% CI for the Median	Variance	SD	SEM	Coefficient of Skewness	Coefficient of Kurtosis	D'Agostino-Pearson Test for Normal Distribution
Normal	201.4839	189.5745 to 213.3932	200.00	180.00 to 214.3918	4488.6095	66.9971	6.0165	0.5557 ($P = 0.0130$)	0.06480 ($P = 0.7425$)	Reject normality ($P = 0.0432$)
Treated	166.0079	158.5448 to 173.4709	164.00	156.9536 to 175.00	1806.1666	42.4990	3.7712	0.3707 ($P = 0.0843$)	0.4247 ($P = 02884$)	Accept normality ($P = 0.1283$)

Struts Width	Arithmetic Mean	95% CI for the Mean	Median	95% CI for the Median	Variance	SD	SEM	Coefficient of Skewness	Coefficient of Kurtosis	D'Agostino-Pearson Test for Normal Distribution
Normal	38.8871	37.5001 to 40.2741	39.00	37.00 to 40.00	60.8815	7.8027	0.07007	0.7598 ($P = 0.0011$)	1.7684 ($P = 0.0064$)	Reject normality ($P = 0.0001$)
Treated	43.7874	42.5887 to 44.9861	43.00	42.00 to 45.032	46.5973	6.8262	0.6057	0.1738 ($P = 0.4086$)	−0.08793 ($P = 0.9598$)	Accept normality ($P = 0.7098$)

Struts Length	Mann-Whitney *U*	*Z* Test	2-Tailed Probability
Normal vs treated	5514.00	4.104	$P < 0.0001$

Struts Width	Mann-Whitney *U*	*Z* Test	2-Tailed Probability
Normal vs treated	4842.00	5.276	$P < 0.0001$

Open cell pore size and interconnection dimensions were calculated with Fiji free software, using Analyze → Measurement function. Data analysis was performed using Med Calc software (Ostend, Belgium). Conditions of normality were checked using D'Agostino-Pearson test. Differences between treated and control groups were assessed using either paired-sample *t* test (for normally distributed data) or Mann-Whitney *U* nonparametric test (for data not following normal distribution).

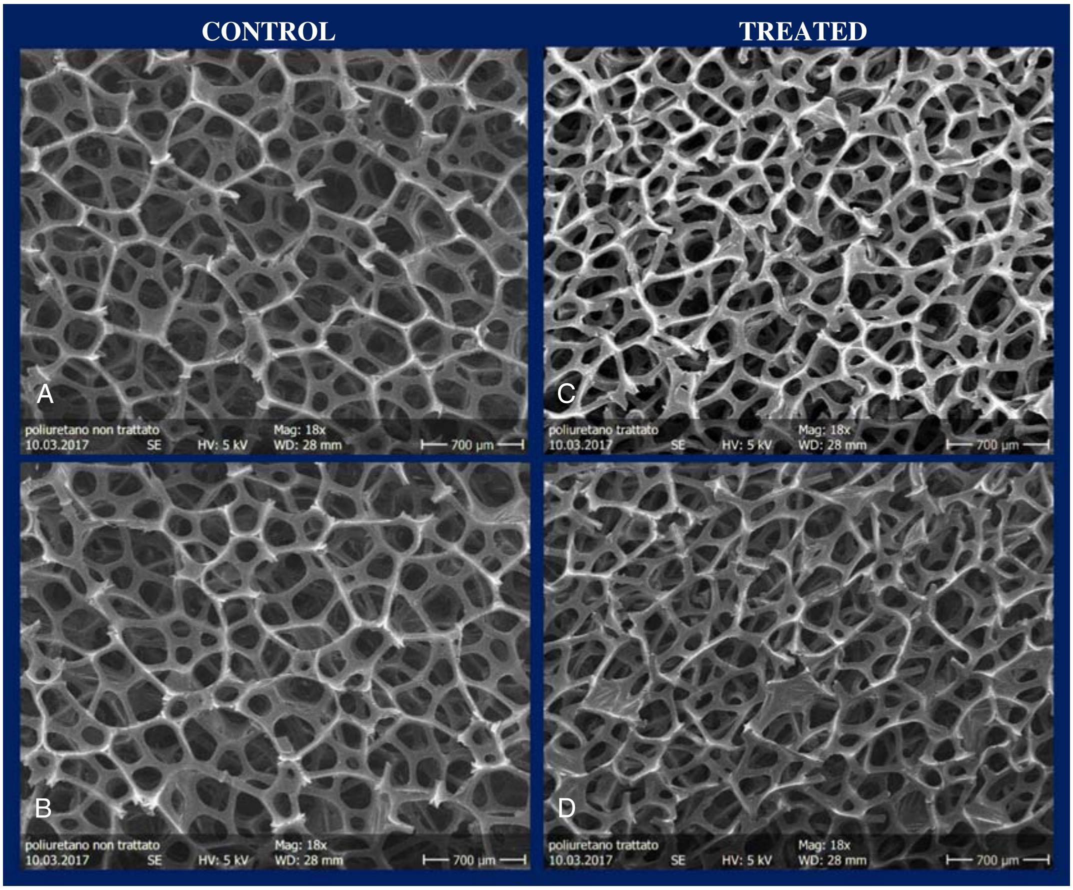

FIGURE 2. Field emission scanning electron microscopy of polyurethane samples. A and B, Control (untreated) polyurethane samples. C and D, Treated polyurethane samples.

profile of normal samples, but there is no information on the spatial frequency of irregularities or the shape of the profile. The other 2 parameters R_{sk} (skewness of the assessed profile) and R_{ku} (kurtosis of the assessed profile) give us important morphological information. The R_{sk} value in the treated samples is higher than that in normal samples, which means that the surface area of the treated samples has a higher number of peaks than the surface area of the untreated samples. The R_{ku} value is higher in the treated samples, which means that the shape of the peaks on the surface of the treated samples is sharper than that of normal samples. Considering the results of the 3 roughness parameters as a whole, we can state that the radiotherapy treatment induces a significant change in the surface morphology of the silicone prosthesis and the height of the profile decreases, and the surface becomes more irregular (rough) due to the presence of a greater number of protrusions and to the sharper shape of the protrusions themselves (Table 1).

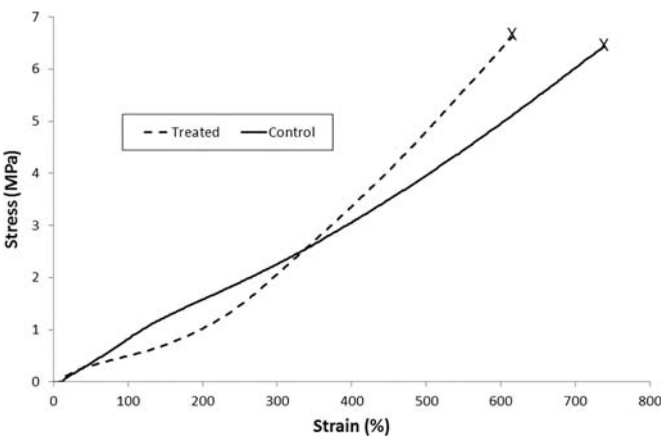

FIGURE 3. Typical stress-strain tensile curves recorded for silicone samples. Breaking point, X.

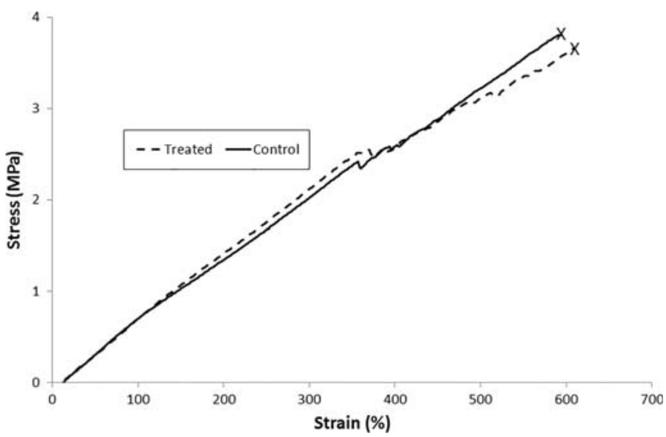

FIGURE 4. Typical stress-strain tensile curves recorded for polyurethane samples. Breaking point, X.

TABLE 3. Tensile Tests

Sample	E_{mod}, MPa	Breaking Strength, MPa	Breaking Strain, %	Thickness, mm	Width, mm
Silicon (control)	0.98	625	734	0.60	2.00
Silicon (treated)	0.38	656	619	0.60	2.00
Polyurethane (control)	0.75	392	581	0.70	2.00
Polyurethane (treated)	0.79	379	614	0.70	2.00

Tensile tests on polyurethane samples showed no significant differences between control and treated conditions. Both treated and control silicone samples revealed, as expected, a marked hyperelastic behavior; thus, their stiffness were described by the elastic modulus, E_{mod}, computed from the initial linear part of the stress-strain curve. In particular, the treated samples exhibited a softer behavior than the control samples until approximately 200% strain and then became quite abruptly stiffer from higher strains until breaking. Treated samples were also characterized by a lower breaking strain but almost the same breaking strength.

Polyurethane implants showed an open cell structure, which closely resembles a sponge. Pore areas and perimeter, together with struts length and thickness, were measured, and results were compared between treated and nontreated samples (Table 2).

Morphological observation of struts from treated sample shows a more compact structure, with significantly shorter and thicker struts compared with normal sample. Shorter struts imply shorter perimeter and narrow area in treated sample (Fig. 2).

The ATR-FTIR spectra of irradiated and control samples were compared either for silicone or polyurethane samples. In the case of silicone-based membranes, treated and control specimens showed similar bands, with little differences in the treated one. In particular, in the irradiated sample, the stretching and bending peaks due to the $Si\text{-}CH_3$ and Si-O-Si bonds are lower in intensity, suggesting an alteration of the polymeric chain. On the contrary, no changes in the ATR-FTIR peaks of the polyurethane samples were observed, suggesting a more stable behavior upon irradiation.

The NMR spectra on the fraction soluble in $CDCl_3$ support these observations, and in the silicone-based sample, upon irradiation, possible esterification processes can be envisaged by the disappearance of the carboxylic signal at approximately 4.0 to 3.2 ppm. The polyurethane sample appeared more stable with respect to the silicone one.

Tensile tests on the polyurethane samples showed no significant differences between control and treated conditions; thus, we now can conclude that the irradiation protocol produced no appreciable effects on the tensile properties of the material (Figs. 3 and 4).

For the silicone samples, both treated and control silicone samples revealed, as expected, a marked hyperelastic behavior; thus, their stiffness were described by the elastic modulus, E_{mod}, computed from the initial linear part of the stress-strain curve. In particular, the treated samples exhibited a softer behavior than the control samples until approximately 200% strain and then became significantly stiffer from higher strains until breaking. Treated samples were also characterized by a lower breaking strain but almost the same breaking strength (Table 3).

DISCUSSION

Breast reconstruction with expanders and implants is one of the most commonly used techniques for breast reconstruction following mastectomy.[13,14] With the increasingly frequent use of radiotherapy as fundamental part of the treatment of breast cancer, plastic surgeons are encountering many more patients who may need PMRT.[15–17] Capsular contracture represents the main complication, resulting in poor expansion, breast distortion, and pain, often requiring additional surgery.[18,19] The pathogenic mechanism is still unknown, but it is certainly a multifactorial process due to the interaction between human body and implant.[20] While the effects of radiation on soft tissues have been deeply investigated, only few studies have examined radiation effects on breast implants.[10] The standard fractionated radiotherapy for breast cancer uses 2-Gy daily fractions for 5 to 6 weeks of treatment. We already studied the alterations of prosthetic implants after standard fractionated radiotherapy in our precedent article.[10] The use of hypofractionated radiotherapy protocol is getting popular over the past decade, leading to less treatment sessions with higher Gy daily doses. In the current study, a multitechnique approach has been pursued to characterize both silicone and polyurethane prosthetic implants in terms of modifications in their surface morphology, mechanical properties, and material chemistry after hypofractionated radiotherapy protocol. In particular, the surface analysis showed deep modifications in the silicone irradiated implant consisting of formation of many secondary and tertiary blebs with heterogeneous dimensions on the top of the primary blebs, whereas the irradiated polyurethane implants showed significantly shorter and thicker struts compared with nonirradiated implant, resulting in a more compact structure.

The ATR-FTIR spectra showed similar bands between silicone irradiated and nonirradiated implants, with little differences in the treated one. In particular, in the irradiated sample, the stretching and bending peaks due to the $Si\text{-}CH_3$ and Si-O-Si bonds were lower in intensity, suggesting an alteration of the polymeric chain. On the contrary, no changes in the ATR-FTIR peaks of the polyurethane samples were observed, suggesting a more stable behavior upon irradiation.

Also, the tensile test demonstrated more variations on silicone implant compared with the polyurethane one. In fact, polyurethane samples showed no significant differences between control and treated conditions.

CONCLUSIONS

Our study investigated with a multitechnique approach the alterations of hypofractionated radiotherapy protocol on silicone and polyurethane implants. Polyurethane implants seem to be more resistant to radiotherapy damage, whereas silicone prosthesis showed more structural, mechanical, and chemical modifications. With our study, we have identified which alterations occur at the implant level without presumption to identify their clinical implications. Certainly, further in vitro studies will be needed to gather evidence on cell-biomaterial interaction phenomena at the surface of irradiated implants.

REFERENCES

1. Whelan TJ, Olivotto I, Ackerman I, et al. NCIG-CTG MA-20: an intergroup trial of regional nodal irradiation in breast cancer. *J Clin Oncol*. 2011. Abstract presented at the 2011 ASCO Annual Meeting.
2. Frasier LL, Holden S, Holden T, et al. Temporal trends in postmastectomy radiation therapy and breast reconstruction associated with changes in National Comprehensive Cancer Network guidelines. *JAMA Oncol*. 2016;2:95–101.
3. Lin KY, Blechman AB, Brenin DR. Implant-based, two-stage breast reconstruction in the setting of radiation injury: an outcome study. *Plast Reconstr Surg*. 2012;129:817–823.
4. Lo Torto F, Parisi P, Casella D, et al. Impact of evolving radiation therapy techniques on implant-based breast reconstruction. *Plast Reconstr Surg*. 2018;141:182e–183e.
5. Moyer HR, Ghazi BH, Losken A. The effect of silicone gel bleed on capsular contracture: a generational study. *Plast Reconstr Surg*. 2012;130:793–800.

6. Ribuffo D, Lo Torto F, Atzeni M, et al. The effects of postmastectomy adjuvant radiotherapy on immediate two-stage prosthetic breast reconstruction: a systematic review. *Plast Reconstr Surg*. 2015;135:445e.
7. Hansen TC, Woeller CF, Lacy SH, et al. Thy1 (CD90) expression is elevated in radiation-induced periprosthetic capsular contracture: implication for novel therapeutics. *Plast Reconstr Surg*. 2017;140:316–326.
8. Kuriyama E, Ochiai H, Inoue Y, et al. Characterization of the capsule surrounding smooth and textured tissue expanders and correlation with contracture. *Plast Reconstr Surg Glob Open*. 2017;5:e1403.
9. Lipa JE, Qiu W, Huang N, et al. Pathogenesis of radiation-induced capsular contracture in tissue expander and implant breast reconstruction. *Plast Reconstr Surg*. 2010;125:437–445.
10. Ribuffo D, Lo Torto F, Giannitelli SM, et al. The effect of post-mastectomy radiation therapy on breast implants: unveiling biomaterial alterations with potential implications on capsular contracture. *Mater Sci Eng C Mater Biol Appl*. 2015;57:338–343.
11. Adamson JD, Cooney T, Demehri F, et al. Characterization of water-clear polymeric gels for use as radiotherapy bolus. *Technol Cancer Res Treat*. 2017;16:923–929.
12. Yildirimer L, Seifalian AM, Butler PE. Surface and mechanical analysis of explanted Poly Implant Prothèse silicone breast implants. *Br J Surg*. 2013;100:761–767.
13. Razdan SN, Cordeiro PG, Albornoz CR, et al. National breast reconstruction utilization in the setting of postmastectomy radiotherapy. *J Reconstr Microsurg*. 2017;33:312–317.
14. Lo Torto F, Cigna E, Kaciulyte J, et al. National breast reconstruction utilization in the setting of postmastectomy radiotherapy: two-stage implant-based breast reconstruction [published online ahead of print August 6, 2017]. *J Reconstr Microsurg*. 2017.
15. Lo Torto F, Vaia N, Casella D, et al. Delaying implant-based mammary reconstruction after radiotherapy does not decrease capsular contracture: an in vitro study. *J Plast Reconstr Aesthet Surg*. 2018;71:28–29.
16. Lo Torto F, Vaia N, Ribuffo D. Postmastectomy radiation therapy and two-stage implant-based breast reconstruction: is there a better time to irradiate? *Plast Reconstr Surg*. 2017;139:1364e–1365e.
17. Meattini I, Saieva C, Marrazzo L, et al. Accelerated partial breast irradiation using intensity-modulated radiotherapy technique compared to whole breast irradiation for patients aged 70 years or older: subgroup analysis from a randomized phase 3 trial. *Breast Cancer Res Treat*. 2015;153:539–547.
18. Nava MB, Pennati AE, Lozza L, et al. Outcome of different timings of radiotherapy in implant-based breast reconstructions. *Plast Reconstr Surg*. 2011;128:353–359.
19. Ascherman JA, Hanasono MM, Newman MI, et al. Implant reconstruction in breast cancer patients treated with radiation therapy. *Plast Reconstr Surg*. 2006;117:359–365.
20. Siggelkow W, Faridi A, Spiritus K, et al. Histological analysis of silicone breast implant capsules and correlation with capsular contracture. *Biomaterials*. 2003;24:1101–1109.

